JURNAL SAINS MATERI INDONESIA (JUSAMI)
ISSN: 1411-1098 (print), 2614-087X (online)
VOL. 27, ISSUE 2, 2026
DOI: https://doi.org/10.55981/jsmi.2026.12209

ORIGINAL ARTICLE

Glucose Detection Using a Surface Plasmon Resonance Biosensor Functionalized by Glucose Oxidase

A. Qonitah[1], A. Udhiarto[1], L. Aprilia[2], S. Pambudi[3] and R. Nuryadi[4]

[1]Electrical Engineering Department, Universitas Indonesia, Indonesia
[2]Research Center for Photonics, National Research and Innovation Agency, Indonesia
[3]Research Center for Vaccine and Drugs, National Research and Innovation Agency, Indonesia
[4]Research Organization for Nanotechnology and Materials, National Research and Innovation Agency, Indonesia

ABSTRACT – Surface plasmon resonance (SPR) is a well-established optical method for biosensing, allowing real-time monitoring of biomolecular interactions without labeling. In this study, an SPR biosensor was designed for glucose detection by modifying a gold (Au) thin film with a self-assembled monolayer (SAM) of 16-mercaptohexadecanoic acid (16-MHA). The SAM layer was chemically activated using (1-ethyl-3-(3-dimethylaminopropyl) carbodiimide hydrochloride /N-hydroxysuccinimide (EDC/NHS), enabling covalent attachment of glucose oxidase (GOx) for selective interaction with glucose molecules. The sensor was tested with glucose solutions (100–300 mM) and corn syrup, which contains both glucose and fructose, to evaluate selectivity. Detection was based on shifts in the resonance angle, which indicate changes in the local refractive index (RI). The Au film/1 mM 16-MHA/GOx sensor exhibited a clear linear correlation between glucose concentration and resonance angle shift. It achieved a sensitivity of 80.5246°/(RIU) or refractive index unit, a full width at half maximum (FWHM) of 2.2426°, a figure of merit (FOM) of 35.9074 RIU^{-1}, and a limit of detection (LOD) of 6.6151 mM, which shows a better performance than the Au film/10 mM 16-MHA/GOx and the bare Au film. Corn syrup produced smaller shifts, confirming the modified sensor's selectivity for β-D-glucose. These results demonstrate the sensor's reliability and selectivity for glucose detection in biomedical applications.

ARTICLE HISTORY
Received: 1 Jul 2025
Revised: 6 Sept 2025
Accepted: 13 Oct 2025

KEYWORDS
Surface plasmon resonance
Glucose sensor
Glucose oxidase
Resonance angle shift
Sensitivity

INTRODUCTION

Glucose is the primary energy source for various bodily functions in humans. Therefore, it is crucial to maintain glucose levels within a normal physiological range. Imbalances in glucose levels, whether low or high, can lead to serious health issues, including diabetes mellitus, one of the most widespread chronic illnesses globally. According to the 11th edition of the International Diabetes Federation (IDF) Atlas, approximately 589 million people aged 20–79 years were living with diabetes in 2024. Indonesia ranked fifth worldwide, with an estimated 20.4 million reported cases [1]. These data underscore the critical importance of regular and accurate glucose monitoring for early detection and prevention of diabetes mellitus and its complications.

Among various optical biosensors, surface plasmon resonance (SPR) is widely used because of its rapid, real-time binding kinetics and high sensitivity [2]. The SPR phenomenon arises when incident light hits free electrons at the interface between a thin metal film, typically gold or silver, and a dielectric medium such as air or a liquid [3]. As a result, this interaction excites the collective oscillations of surface electrons (surface plasmons). It produces a sharp dip in the reflected light intensity at a specific angle, known as the resonance angle, where reflectivity reaches its minimum [4], [5]. In contrast to fluorescence-based assays, SPR enables label-free monitoring of biomolecular interactions by detecting changes in the local refractive index (RI) near the metal surface, which are observed as shifts in the resonance angle [6]. Biological recognition elements such as enzymes, antibodies, or DNA can be immobilized on the sensor surface to provide selective detection. With these capabilities, SPR offers highly sensitive detection in biomedical applications, ranging from cervical cancer screening [7], virus detection [8] to body fluid analysis, including glucose monitoring [9].

Hsieh et al. [9] demonstrated an SPR biosensor using genetically modified glucose/galactose-binding protein (GGBP) as the sensing element, which was immobilized via thiol-based chemistry. Although their method enabled glucose detection, the non-enzymatic nature of the bioreceptor limited its specificity. Other studies have explored non-enzymatic glucose detection using advanced nanomaterials, such as pristine and modified UiO-66 frameworks [10], $MoSe_2$/ZnO composites [11], and MoS_2-graphene hybrids [12]. These materials enhanced sensitivity, but their costly synthesis and complex surface modifications limit their practical use for routine glucose monitoring. Our previous work also performed

***CORRESPONDING AUTHOR** | A. Qonitah; A. Udhiarto; L. Aprilia | ✉ atikah.qonitah@ui.ac.id; arief.udhiarto@ui.ac.id; lia.aprilia@brin.go.id

direct glucose detection using SPR without enzyme functionalization, which achieved reasonable sensitivity but suffered from cross-reactivity with other sugars [13], [14].

To address this limitation, an SPR biosensor functionalized with glucose oxidase (GOx) was developed, as GOx specifically catalyzes the oxidation of β-D-glucose. This reaction produces local RI changes that appear as measurable shifts in the attenuated total reflection (ATR) curve [15]–[17]. A gold (Au) thin film was modified with 16-mercaptohexadecanoic acid (16-MHA) and then activated with 1-ethyl-3-(3-dimethylaminopropyl)carbodiimide hydrochloride/N-hydroxysuccinimide (EDC/NHS) to covalently immobilize GOx. Since the density and orientation of enzymes are influenced by the ratio of alcohol-terminated (–OH) to carboxylic acid-terminated (–COOH) thiols [18], 16-MHA was selected for its –COOH group and long n-alkanethiol chain, which helps ensure effective enzyme spacing and stable covalent binding. Finally, the sensor's selectivity was assessed by comparing responses to glucose solutions and corn syrup, which contains both glucose and fructose.

EXPERIMENTAL METHOD

Materials

The buffered solutions of 2-(N-morpholino)ethanesulfonic acid (MES, ≥99%, Himedia) and phosphate-buffered saline tablets (PBS, pH 7.2, Sigma-Aldrich) were prepared for functionalization and assay solutions. Organic solvents, including acetone, ethanol, and 2-propanol (all EMSURE® ACS, ISO grade, Supelco), were used for gold (Au) thin film cleaning and preparation processes. 16-mercaptohexadecanoic acid (16-MHA, 90%, Sigma-Aldrich) was used for self-assembled monolayer (SAM) layer formation. Surface activation was achieved with 1-ethyl-3-(3-dimethylaminopropyl)carbodiimide (EDC, Thermo Fisher Scientific) and N-hydroxysuccinimide (NHS, 98%, Sigma-Aldrich). D-(+)-Glucose (≥99.5%, Sigma-Aldrich) was the target analyte, while corn syrup containing glucose and fructose (Daesang Corporation) was tested to evaluate selectivity. The glucose oxidase enzyme (GOx, 100,000-250,000 units/g solid, Sigma-Aldrich) was the bio-recognition element in the functionalization process and was immobilized as the ligand on the Au surfaces.

Methods and Procedures

Pre-treatment and Cleaning of Au Thin Films

Cleaning and pre-treatment of the Au thin films are crucial for achieving the formation of a high-quality SAM and maximizing the immobilization density of biomolecules. A previous study has demonstrated that cleaning with organic solvents enhances the GOx loading density on Au thin films [18]. Furthermore, oxygen plasma treatment improves the surface transducer performance compared with traditional methods, such as piranha and potassium hydroxide (KOH) solutions [19].

In the cleaning process, Au thin films were first soaked in acetone solution for 10 minutes to remove organic contaminants, followed by sequential immersion in ethanol and 2-propanol (isopropanol) solutions for 2 minutes each to ensure thorough cleaning [18]. The substrates were then rinsed with deionized (DI) water to remove residual chemicals and dried using nitrogen gas. Finally, the substrates were exposed to ozone plasma at 100 watts for 10 minutes to enhance their surface quality and bio-functionalization [19], [20]. This cleaning process was crucial for preparing Au thin films for subsequent SAM formation and functionalization, thereby maintaining the optimal surface quality for biomolecular interactions.

Self-assembled Monolayer, Carboxylation, and GOx Immobilization

To facilitate the immobilization of GOx on the Au thin films, a carboxyl-terminated SAM was prepared and subsequently activated using EDC/NHS, as the scheme is illustrated in Figure 1. This approach enables covalent bonding between the enzyme and surface via esterification, where the lysine residues of GOx displace the NHS group on the activated carboxylate-terminated SAM [18]. Covalent bonding ensures stable and robust immobilization of GOx, which is critical for reliable biosensor performance.

The cleaned Au substrates were incubated in 16-MHA solution in ethanol at room temperature to form the SAM layer through Au–S bonds. The substrates were sequentially rinsed with ethanol and DI water to remove unbound molecules and then dried with nitrogen gas. The SAM-modified substrates were immersed in an activation solution containing 4 mM EDC and 1 mM NHS in 5 mL of 100 mM MES buffer (pH 5.5) for 30 minutes to activate the carboxylic acid groups (-COOH). Following activation, the substrates were rinsed with MES buffer and dried in nitrogen gas.

For enzyme immobilization, the activated substrates were incubated overnight (12–18 hours) at ~4°C in GOx (10 mg/mL) prepared in 5 mL of 0.05 M PBS solution. After incubation, the substrates were rinsed with PBS solution to remove unbound GOx and dried with nitrogen gas. This procedure ensures high-density and stable immobilization of GOx on Au substrates, optimizing the biosensor's sensitivity and specificity for glucose detection.

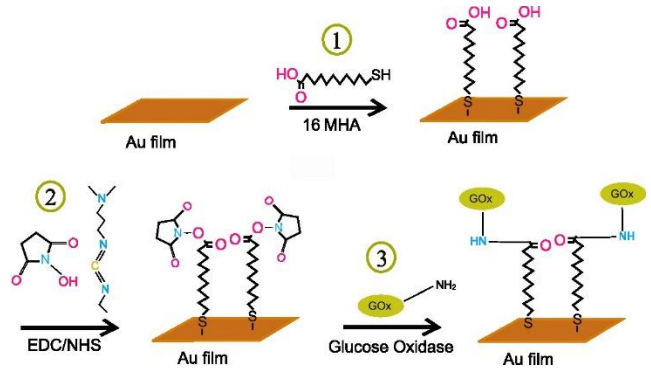

Figure 1. Illustration of the Au thin film functionalization process

Preparation of Glucose and Corn Syrup Analyte Solutions

The required amounts of glucose (M_r = 180.16 g/mol) were calculated and weighed to prepare 30 mL solutions at concentrations of 100, 200, and 300 mM. Each was transferred into a volumetric flask and diluted with 30 mL of 0.05 M PBS solution. Similarly, corn syrup (M_r = 180 g/mol) solutions were prepared at the same concentrations by accurately weighing the required mass and dissolving it in DI water with gentle shaking until homogeneous, yielding 30 mL for each concentration. These solutions were used for the selectivity test.

The glucose solutions were allowed to equilibrate at room temperature for a minimum of 12 hours prior to experimental application. This equilibration step was crucial for stabilizing the proportion between β-D-glucose and α-D-glucose, thereby minimizing measurement errors. Achieving this dynamic equilibrium is essential for glucose detection applications, as it ensures the availability of β-D-glucose, which is the specific substrate of GOx [17]. GOx is widely employed in glucose detection because of its strong affinity for β-D-glucose. In the catalytic reaction, GOx serves as a catalyst for the oxidation of β-D-glucose into β-D-gluconolactone (D-glucono-1,5-lactone), while concurrently reducing molecular oxygen to hydrogen peroxide (H_2O_2), as in Equation (1):

$$\beta\text{-}D\text{-}glucose + H_2O + O_2 + GOx \rightarrow \beta\text{-}D\text{-}gluconolactone + H_2O_2 \quad (1)$$

Measurement

The experimental apparatus utilized the NanoSPR-6, BA1000 system, which comprised a fixed 650-nm semiconductor laser, a stepping motor, a glass prism (n=1.61), and photodiode detectors. The Au thin film was a commercial surface plasmon resonance (SPR) substrate (NanoSPR-6) with a 5 nm chromium (Cr) adhesion layer and a 45 nm Au layer on a 20×20 mm glass slide, annealed for 30 minutes [21]. As illustrated in Figure 2, the sensor was set up in the Kretschmann configuration with a glass prism, Au thin film, GOx immobilization layer, and analyte as the sensor interface. The functionalized Au thin film was mounted on the prism. A silicon gasket and cuvette were installed on the substrate, and the microfluidic system was connected via a rubber tube to a bio-minipump, which controlled the flow of the analyte solution across the Au substrate chamber.

A p-polarized laser beam is directed at the Au surface from a high refractive index medium (such as a glass prism), producing total internal reflection (TIR) and generating an evanescent wave at the metal-dielectric interface. When the wave energy matches the natural oscillation of free electrons on the Au surface, surface plasmon oscillations are excited [22]. Under the resonance condition, the incident-light frequency aligns with the plasmon frequency, resulting in a decrease in reflectance at the SPR angle. The evanescent field decays within a depth of approximately 50–300 nm from the sensor surface and facilitates sensitive interactions with molecules in close proximity. However, this limits its applicability in measurements that require either extremely narrow detection ranges or long-range interactions [23], [24]. This penetration depth allows the detection of refractive index (RI) changes in the surrounding medium, which are detected by the photodiodes and recorded as graphical changes in reflectance and resonance angle. In this experiment, the measurements were performed in the kinetic mode, where the analytes are monitored in real-time.

In analyte measurement, solutions with different concentrations (100, 200, and 300 mM) were measured, as well as the corn syrup solutions. The PBS solution was first flowed as a reference or baseline, passing through a peristaltic pump to fill the chamber on the functionalized Au film. Each analyte concentration was measured alternately with the baseline at a certain time.

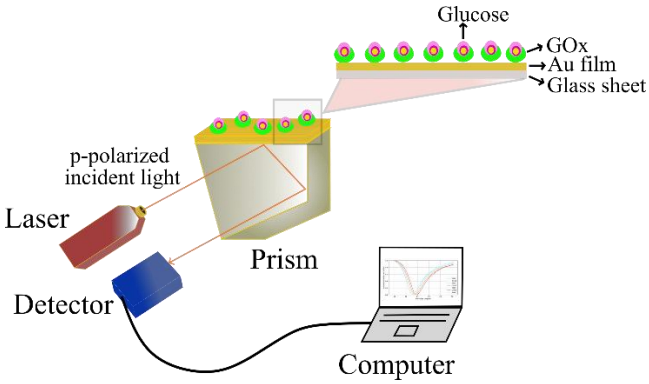

Figure 2. Schematic of experimental setup

RESULTS AND DISCUSSION

Effect of 16-MHA Concentration on Self-Assembled Monolayer (SAM) for Glucose Detection

This study examined the impact of different 16-mercaptohexadecanoic acid (16-MHA) concentrations (1 mM and 10 mM) on the kinetics of gold (Au) thin film self-assembly using surface plasmon resonance (SPR). The objective was to analyze the resulting SPR angle shifts and evaluate the effects of concentration and incubation time on monolayer formations. Subsequently, the resulting SAMs were activated with (1-ethyl-3-(3-dimethylaminopropyl) carbodiimide hydrochloride/N-hydroxysuccinimide (EDC/NHS) and functionalized with glucose oxidase enzyme (GOx), and the SPR angle shifts in response to various glucose concentrations were evaluated to assess how different SAM conditions influence the refractive index (RI) changes at the sensor interface.

SPR Observation of 16-MHA formation

Self-assembly was conducted in ethanol solutions containing 16-MHA at 1 mM and 10 mM concentrations. The Au substrates were alternately mounted within a cuvette and immersed in 16-MHA solutions for self-assembly during in situ SPR measurements. The process lasted approximately 3 hours for both concentrations. After immersion, the substrates were rinsed with a continuous ethanol stream for 15 minutes to remove the unbound thiol molecules.

Real-time SPR measurements during 16-MHA adsorption revealed distinct self-assembly kinetics at each concentration. The SPR angle shift kinetics are illustrated in Figure 3 and Figure 4, where the x-axis represents the immersion time of the 16-MHA solution. Figure 3 illustrates the SPR response for 1 mM 16-MHA, showing a larger SPR angle shift of approximately 2.03° within the initial 60 minutes, which suggests the possibility of faster and more efficient monolayer formation on the Au surface. A smaller shift of around 1.11° was observed between 60 and 180 minutes, indicating that the SAM had reached saturation. In contrast, Figure 4 shows the SPR response for 10mM 16-MHA, where the angle shift is smaller and increases more slowly. This behaviour indicates less efficient layer formation, likely due to denser molecular interactions at higher 16-MHA concentration, which may have hindered effective thiol adsorption and organized self-assembly on the Au surface. Thus, 1 mM was selected for subsequent GOx functionalization owing to its faster and more efficient monolayer formation. This concentration is expected to enhance the GOx immobilization efficiency and maintain optimal sensor performance. An incubation time of 60 minutes was sufficient to form a stable SAM layer without the risk of excessive thickness. Prolonged incubation may lead to multilayer formation or surface defects instead of a uniform monolayer, potentially hindering analyte-ligand interactions and reducing binding efficiency [25]. As a result, it adversely affects the overall sensor performance rather than enhancing sensitivity.

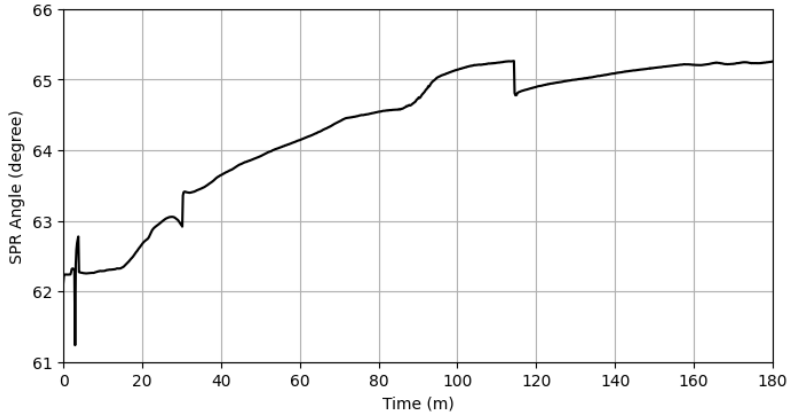

Figure 3. Real-time SPR curve of 16-MHA (1 mM) layer formation on the Au surface

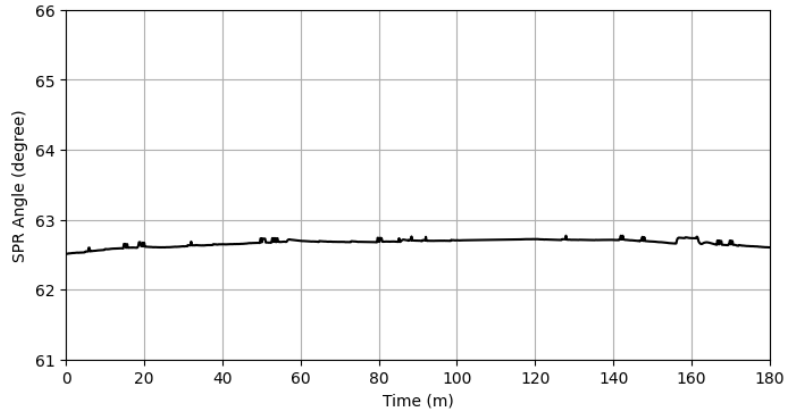

Figure 4. Real-time SPR curve of 16-MHA (10 mM) layer formation on the Au surface

Glucose Detection

The SPR-based glucose detection was investigated using Au films modified SAM with 1 mM and 10 mM 16-MHA, followed by the immobilization of GOx, with a bare Au film included as a negative control. Figure 5 and Figure 6 show the real-time SPR response to sequential injections of glucose solutions at concentrations of 100 mM, 200 mM, and 300 mM. A progressive increase in the resonance angle was observed as the glucose concentration increased. This reflects RI changes at the sensor interface caused by enzymatic glucose oxidation. The injection of phosphate-buffered saline (PBS) solution between glucose measurements effectively regenerated the baseline. Although the injection direction differed between the two experiments, this variation did not affect the SPR angle or its shift, as each measurement was baseline-corrected using PBS achieved before analyte injection.

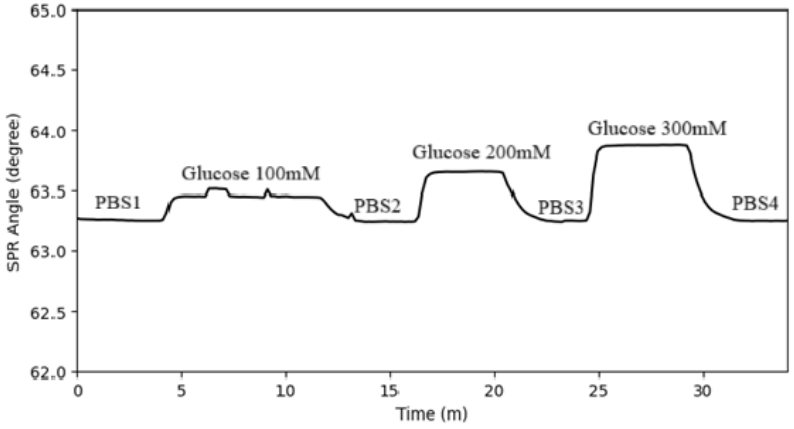

Figure 5. Real-time curve of glucose detection on Au-film/16-MHA (1mM)/GOx

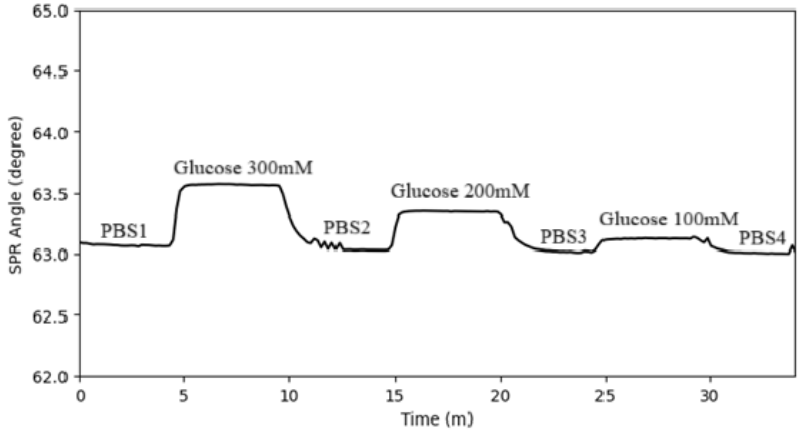

Figure 6. Real-time curve of glucose detection on Au-film/16-MHA (10mM)/GOx

As shown in Figure 7, the real-time response curves display two distinct phases. The association phase occurs when glucose molecules bind to immobilized GOx, while the dissociation phase begins when PBS is introduced to wash away unbound molecules. Quantitative kinetic analysis based on the 1:1 Langmuir interaction model, as reported in [26], showed that the Au film/1 mM 16-MHA/GOx exhibited a higher association rate constant ($k_a = 0.2849\ M^{-1}s^{-1}$) and a slightly higher dissociation rate constant ($k_d = 0.0239\ s^{-1}$) compared to the Au film/10 mM 16-MHA/GOx ($k_a = 0.1476\ M^{-1}s^{-1}$, $k_d = 0.0191\ s^{-1}$). The resulting equilibrium dissociation constant ($K_D = {k_d}/{k_a}$) was lower for the substrate with 1 mM 16-MHA (0.084 M) than for the 10 mM 16-MHA (0.1296 M), indicating a stronger overall binding affinity between glucose and the GOx-functionalized surface at the lower SAM concentration. These results indicate that a less densely packed monolayer improves glucose access to GOx active sites, which enhances both the interaction rate and overall binding strength. These kinetic findings align with the Langmuir binding model commonly applied in SPR biosensing, where a higher k_a and a lower K_D reflect faster and stronger binding interactions [26].

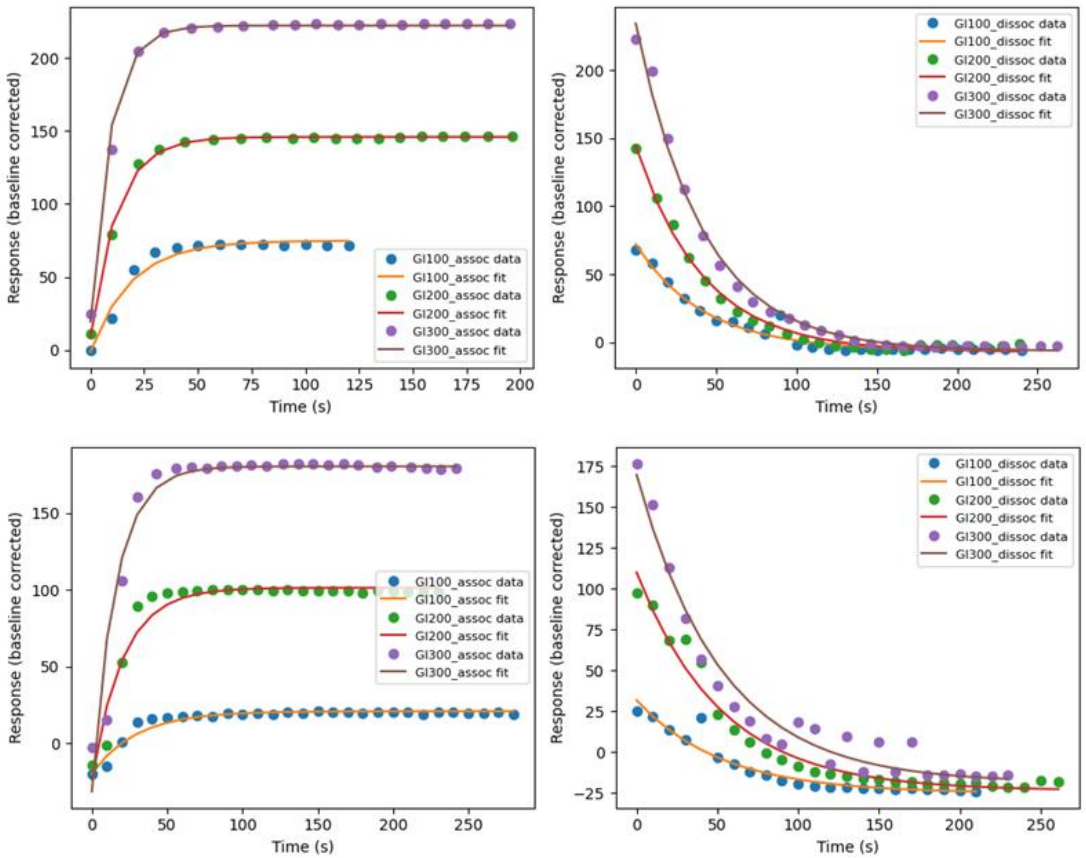

Figure 7. Kinetic curves for Au film/16-MHA/GOx at two SAM concentrations: (a) association and (b) dissociation phases for 1 mM 16-MHA; (c) association and (d) dissociation phases for 10 mM 16-MHA

Figure 8 and Figure 9 illustrate the angular shift through the attenuated total reflection (ATR) reflectance curves derived from the real-time data in Figure 5 and Figure 6. Each glucose concentration produced a distinct resonance angle at the minimum reflectance. This behavior is consistent with the sensing mechanism of glucose detection using GOx, as in Equation (1), where the enzymatic oxidation of β-D-glucose to β-D-gluconolactone and hydrogen peroxide alter the local refractive index near the sensor surface. As β-D-glucose binds to the flavin adenine dinucleotide (FAD) coenzyme in GOx, the local refractive index changes proportionally with glucose concentration, resulting in measurable shifts in the SPR resonance angle. Therefore, the observed angular shifts directly reflect the enzymatic interaction between β-D-glucose and immobilized GOx [15].

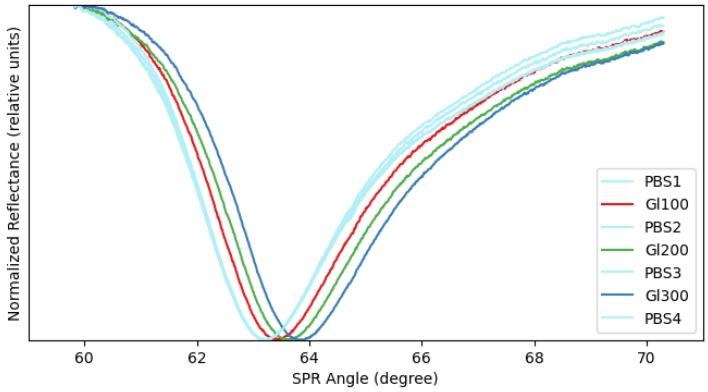

Figure 8. ATR curve of glucose detection on Au-film/16-MHA (1mM)/GOx

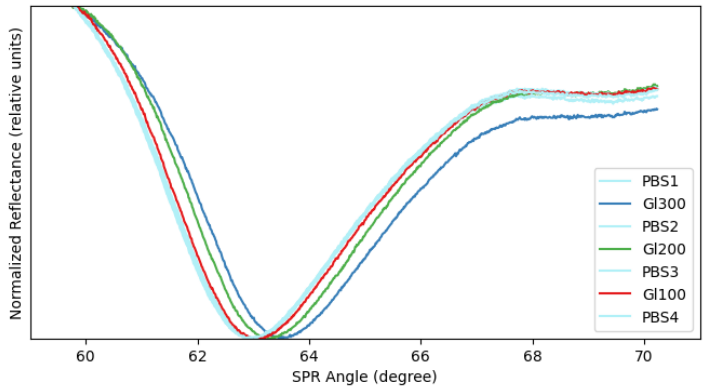

Figure 9. ATR curve of glucose detection on Au-film/16-MHA (10mM)/Gox

As shown in Figure 10, a clear linear correlation was observed among the three substrates. The Au film/1 mM 16-MHA/GOx consistently showed larger resonance angle shifts across all tested glucose concentrations compared to the Au film/10 mM 16-MHA/GOx and bare Au film. The highest SPR angle shift observed on the Au film/1 mM 16-MHA/GOx suggests a more effective RI change upon glucose interaction with GOx, indicating better enzymatic activity at the lower SAM concentration. This enhanced response results from the lower density of 16-MHA at 1 mM, which enables the formation of a thin and uniform SAM monolayer. Consequently, GOx is optimally immobilized through covalent binding with 16-MHA, thereby facilitating easier access of glucose molecules to the enzyme's active sites. At a higher 16-MHA concentration (10 mM), the SAM layer becomes denser and potentially less uniform, leading to suboptimal GOx immobilization and reduced glucose interaction. A very thick layer may position GOx beyond the evanescent field penetration depth, limiting the SPR response to analyte-ligand interactions [27]. In our study, this corresponds to β-D-glucose catalyzed by GOx. This trend aligns with report of other thiol-based biosensors, where excessive surface coverage causes steric hindrance and restricts analyte transport, reducing the overall signal. It has been emphasized that a thinner and uniformly distributed thiol layer is essential for improved sensitivity [28].

Linear regression is used to examine the relationship between the SPR angle shift ($\Delta\theta_{SPR}$) and glucose concentration. The analysis produced regression equations of $\Delta\theta_{SPR} = 0.0021\text{x} - 0.012$ ($R^2 = 0.9987$) for the Au film/1 mM 16-MHA/GOx, $\Delta\theta_{SPR} = 0.002\text{x} - 0.0893$ ($R^2 = 1$) for the Au film/10 mM 16-MHA/GOx, and $\Delta\theta_{SPR} = 0.0022 - 0.0761$ ($R^2 = 0.9998$) for the bare Au film. Although the linear regression slopes show slightly lower sensitivity than the bare Au film, the Au film/1 mM 16-MHA/GOx exhibited the largest SPR angle shifts at the tested glucose concentrations. This reflects enhanced specific interaction between β-D-glucose and GOx. All R^2 values were greater than 0.99, indicating a highly linear response for reliable performance of the sensor.

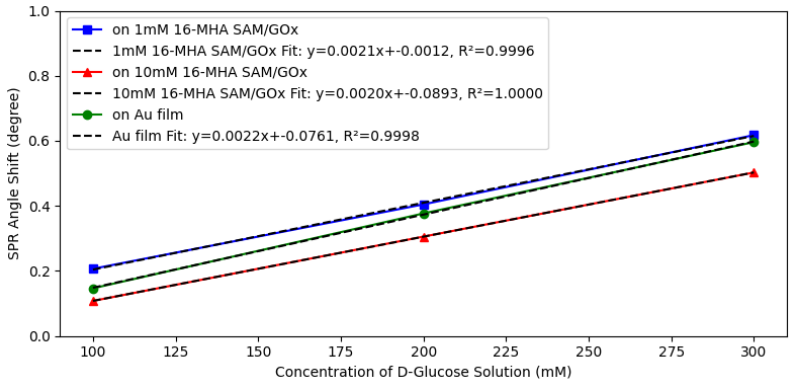

Figure 10. Comparison of SPR angle shift versus glucose concentration for Au film (green), Au film with 16-MHA 1 mM/GOx (blue), and 16-MHA 10 mM/GOx (red)

Comparison of Glucose and Corn Syrup Detection

Figure 11 shows the resonance angle shift in response to the glucose standard solution and corn syrup solution (with similar concentrations). In this case, corn syrup contains half glucose and half fructose, so the glucose concentration in corn syrup is less than in the glucose standard solution. The SPR angle shift for glucose was higher at all glucose concentrations than for corn syrup detection. The results indicated that glucose interacts more specifically and efficiently with GOx, so the solution containing more glucose results in a larger and clearer SPR signal change.

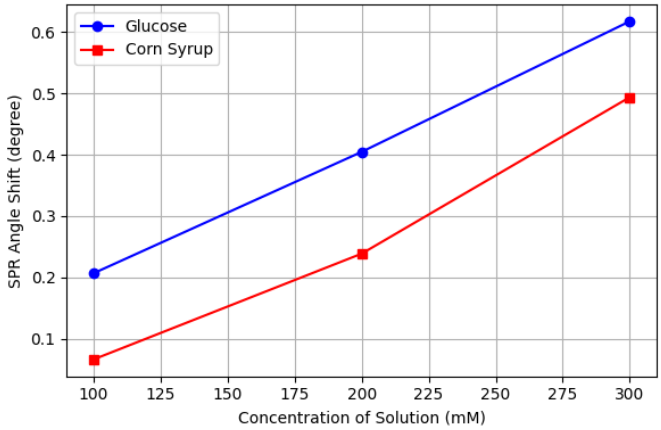

Figure 11. SPR angle shift for the glucose solution (blue) and corn syrup solution (red)

Evaluation of SPR Performance

Several fundamental parameters are commonly assessed for SPR sensor performance, including sensitivity (S), full width at half maximum (FWHM), figure of merit (FOM), and limit of detection (LOD). To achieve optimal sensor functionality, the S and FOM values should ideally achieve the highest possible values. These metrics can be determined using Equation (2) and Equation (3). A higher S value indicates greater sensor responsiveness to small changes in the RI. The correlation between S and the shift in resonance angle is as outlined in Equation (2), which is defined by comparing the SPR resonance angle shift ($\Delta\theta_{SPR}$) to the change in the RI of the analyte (Δn). $\Delta\theta_{SPR}$ represents the change in the resonance angle before (baseline) and after glucose interacts with the functionalized sensor surface and Δ_n corresponds to the variation in the RI of the medium in contact with the SPR-active surface. In addition, the FOM is inversely proportional to FWHM. The FWHM value can be determined from the reflectance depth ($\Delta\theta_{0.5}$), which represents the width of the SPR reflectance curve. A smaller FWHM indicates more specific and accurate detection of resonance angle shifts. Therefore, it is essential to maintain a minimal FWHM value because the FOM is highly dependent on the calculation (3) [22], [29]. In addition, the LOD was evaluated to quantify the smallest analyte concentration that can be detected by the sensor, which is closely related to the overall sensitivity of the system [30]. The LOD is defined as the analyte concentration that produces a signal equal to three times the standard deviation of the blank measurement, as shown in (4) [31], [32]. In this study, the slope was obtained from the linear regression of θ_{SPR} against the analyte concentration (mM), while the standard deviation (σ_{blank}) was estimated from baseline noise using resonance angle fluctuations observed during repeated PBS injections without analyte.

$$S = \frac{\Delta\theta_{SPR}}{\Delta n} \quad (2)$$

$$FOM = \frac{S}{FWHM} \quad (3)$$

$$LOD = \frac{3 \times \sigma_{blank}}{\text{slope}} \quad (4)$$

The comparative performance results (S, FWHM, and FOM) of the GOx-functionalized Au films and the bare Au film for glucose and corn syrup detection at each analyte concentration are summarized in Tables 1 and 2. The refractive indices of glucose and corn syrup solutions at different concentrations were measured directly using a refractometer to ensure the accuracy of the ΔRI values used in the analysis. As shown in Table 1, the Au film/1 mM 16-MHA/GOx shows the best performance compared to the bare Au film and the Au film/10 mM 16-MHA/GOx, with higher sensitivity (S), a narrower resonance peak (smaller FWHM), and a higher FOM. In contrast, the 10 mM SAM configuration exhibits lower sensitivity than the bare Au film, suggesting that an excessively dense SAM layer can reduce sensor performance, in some cases even below that of the bare Au film. When the same 1 mM 16-MHA/GOx substrate is used to compare glucose and corn syrup detection, as shown in Table 2, glucose generates a sharper resonance peak with a smaller FWHM. This is due to the specific and localized interaction between glucose and GOx, while corn syrup, which consists of a mixture of glucose and fructose, produced a broader and less focused response. As a result, the FOM for glucose detection was higher, whereas the FOM for corn syrup was lower, highlighting the sensor's specificity toward glucose. These findings emphasize the importance of selecting an appropriate SAM density (concentration) to balance sensitivity and specificity in glucose detection.

Moreover, the LOD values further support the significant improvement in the detection capability. The 1 mM 16-MHA/GOx substrate achieves the lowest LOD of 6.6151 mM, with $\sigma_{blank} = 0.0045°$, compared to 39.7403 mM ($\sigma_{blank} = 0.0251$ °) for the 10 mM 16-MHA/GOx substrate and 42.289 mM ($\sigma_{blank} = 0.0285$ °) for the bare Au film. The LOD of 6.6151 mM corresponds to approximately 119.18 mg/dL, which is much higher than the ±15 mg/dL accuracy threshold specified by ISO 15197:2013 for commercial glucose meters [33]. However, this functionalized SPR sensor is still at an early development stage; therefore, direct comparison with commercial devices is not appropriate. Further validation using biological matrices at physiologically relevant glucose concentrations is needed to assess its potential for clinical diagnostic applications.

Table 1. SPR performance in glucose detection

Analyte Solution (mM)	RI (n)	Performance Parameters (Au film/1mM 16-MHA/GOx)			Performance Parameters (Au film/10mM 16-MHA/GOx)			Performance Parameters (Au film)		
		*S (°/**RIU**)*	*FWHM (°)*	*FOM (**RIU**$^{-1}$)*	*S (°/**RIU**)*	*FWHM (°)*	*FOM (**RIU**$^{-1}$)*	*S (°/**RIU**)*	*FWHM (°)*	*FOM (**RIU**$^{-1}$)*
PBS	1.3331	-	-	-	-	-	-	-	-	-
Glucose 100	1.3357	80.1376	2.1625	37.0584	41.8570	2.4108	17.3624	57.7965	3.1853	18.1446
Glucose 200	1.3382	79.3555	2.1535	36.8489	59.9229	2.3875	25.0990	77.3900	3.4965	22.1334
Glucose 300	1.3408	80.5246	2.2426	35.9074	65.5400	2.3148	28.3136	81.0344	3.4781	23.2987

Table 2. SPR performance in corn syrup detection

Analyte Solution (mM)	RI (n)	Performance Parameters (Au film/1mM 16-MHA/GOx)		
		*S (°/**RIU**)*	*FWHM (°)*	*FOM (**RIU**$^{-1}$)*
Aquabidest	1.331	-	-	-
Corn Syrup 100	1.3343	7.1049	2.0453	3.4738
Corn Syrup 200	1.3362	45.8307	2.2062	20.7737
Corn Syrup 300	1.3382	68.8853	2.2106	31.0638

CONCLUSION

Glucose detection using surface plasmon resonance (SPR) functionalized with glucose oxidase (GOx) through a self-assembled monolayer (SAM) of 1 mM 16-mercaptohexadecanoic acid (16-MHA) is successfully demonstrated, with the 1 mM concentration showing better performance than the 10 mM concentration. Observations from the SAM method indicate that the lower concentration (1 mM) forms a well-structured monolayer more readily, allowing for uniform and rapid coverage. Consequently, when this concentration was used to functionalize GOx on the gold (Au) film for glucose detection, the substrate (Au film/1 mM 16-MHA/GOx) exhibited higher sensitivity compared to the Au film/10 mM 16-MHA/GOx and even the bare Au film. When tested for selectivity with corn syrup, which contains both glucose and fructose, the Au film/1 mM 16-MHA/GOx showed higher SPR angle shifts for glucose, and the calculated performance parameters confirm its selectivity. The glucose measurement yielded higher sensitivity ($80.5246°/RIU$), narrower FWHM ($2.2426°$), superior FOM ($35.9074\ RIU^{-1}$) and lower LOD (6.6151 mM), highlighting its improved performance. These results demonstrate that SPR functionalized with GOx, using 16-MHA as a linker atconcentration of 1 mM, provides effective covalent binding and improved sensor performance for glucose detection. This indicates the sensor's reliability and selectivity for glucose monitoring in biomedical applications. Future work will focus on evaluating the stability of the sensor, testing selectivity against other common interfering substances (e.g., sucrose, galactose, fructose), and assessing performance in non-invasive samples such as saliva at physiologically relevant glucose concentrations.

ACKNOWLEDGEMENT

This work received partial support from the "Rumah Program" research grant, awarded by the Research Organization for Nanotechnology and Materials, National Research and Innovation Agency (BRIN), in 2025.

REFERENCES

[1] International Diabetes Federation (IDF) Diabetes Atlas. "The global picture of diabetes," 11th ed., chap. 3, 2025, pp. 42–48.

[2] T. Chen, J. Xin, S. J. Chang, C. Chen, and J. T. Liu. "Surface Plasmon Resonance (SPR) Combined Technology: A Powerful Tool for Investigating Interface Phenomena." *Advanced Materials Interfaces*, vol. 10, no. 8, pp. 2202202, 2023.

[3] T. Deka and R. G. Nair. "Recent Advancements in Surface Plasmon Resonance and Schottky Junction Assisted Photocatalytic Water Splitting Of Noble Metal Decorated Titania: A Review." *International Journal of Hydrogen Energy*, vol. 59, pp. 322–342, 2024.

[4] R. Nuryadi, R. D. Mayasari, L. Aprilia, and B. Yuliarto. "Fabrication Of ZnO/Au/Prism-Based Surface Plasmon Resonance Device for Gas Detection," in *2015 International Conference on Quality in Research (QiR)*, Lombok, Indonesia, pp. 26–29, 2015.

[5] R. Nuryadi and R.D. Mayasari. "ZnO/Au-Based Surface Plasmon Resonance for CO_2 Gas Sensing Application." *Appl. Phys. A, vol.* 122, no. 33, 2016.

[6] H. H. Nguyen, J. Park, S. Kang, M. Kim. "Surface Plasmon Resonance: A Versatile Technique for Biosensor Applications." *Sensors*, vol. 15, no. 5, pp. 10481–10510, 2015.

[7] T. Kamani, S.K. Patel, N. K. Anushkannan, S. B. Khalifa, S. Chebaane, and T. Saidani. "Design and Development of Surface Plasmon Resonance Biosensor for Early Detection of Cervical Cancer Utilizing Nucleus and Cytoplasm." *Plasmonics*, 2024.

[8] V. Kumar, R. Kumar, S. Pal, and Y.K. Prajapati. "Development of Surface Plasmon Resonance Sensor Utilizing Gase and WS2 for Ultra-Sensitive Early Detection of Dengue Virus." *Optics*, vol. 313, p.171975, 2024.

[9] H. V. Hsieh, Z. A. Pfeiffer, T. J. Amiss, D. B. Sherman, and J. B. Pitner. "Direct Detection of Glucose by Surface Plasmon Resonance with Bacterial Glucose/Galactose-Binding Protein." *Biosensors and Bioelectronics,* vol. 19, no. 7, pp. 653–660, 2004.

[10] G. Gumilar, J. Henzie, B. Yuliarto, A. Patah, N. Nugraha, M. Iqbal, M. A. Amin, M. S. A. Hossain, Y. Yamauchi, and Y. V. Kaneti. "Performance Enhancement Strategies for Surface Plasmon Resonance Sensors in Direct Glucose Detection Using Pristine and Modified Uio-66: Effects of Morphology, Immobilization Technique, and Signal Amplification." *J. Mater. Chem. A,* vol. 10, no. 12, pp. 6662–6678, 2022.

[11] R. Chen, C. Guo, G. Lan, P. Luo, J. Yi, and W. Wei. "Highly Sensitive Surface Plasmon Resonance Sensor with Surface Modified MoSe2/ZnO Composite Film for Non-Enzymatic Glucose Detection." *Biosensors and Bioelectronics,* vol. 237, p. 115469, 2023.

[12] H. Yu, Y. Chong, P. Zhang, J. Ma, and D. Li. "A D-Shaped Fiber SPR Sensor with a Composite Nanostructure of Mos 2-Graphene for Glucose Detection." *Talanta*, vol. 219, p. 121324, 2020.

[13] A. Qonitah, L. Aprilia, I. Darmadi, W. P. Tresna and R. Nuryadi, "Observation of Glucose Concentration in Water using Surface Plasmon Resonance," in *2023 International Conference on Radar, Antenna, Microwave, Electronics, and Telecommunications (ICRAMET)*, Bandung, Indonesia, pp. 226–230, 2023.

[14] L. Aprilia, D. Riana, W.P. Tresna, I. Tazi, and R. Nuryadi, "Surface Plasmon Resonance (SPR) Sensor for Measurement of Glucose and Ethanol Concentrations," in *AIP Conf. Proc*. 3003, p. 020106, 2024.

[15] W. Zheng, B. Han, S. E, Y. Sun, X, Li, Y. Cai, and Y. Zhang. "Highly-Sensitive and Reflective Glucose Sensor Based on Optical Fiber Surface Plasmon Resonance." *Microchemical Journal*, vol. 157, p. 105010, 2020.

[16] W. Fang, L. Ding, Y. Zhang, and H. Li, "Prism SPR Glucose Sensor Based on Gold Nanoparticle/Gold Film Coupling Enhanced SPR." *IEEE SENSORS JOURNAL*, vol. 23, no. 12, 2023.

[17] Pine Research Instrumentation, "Electrochemical-Enzymatic Determination of Glucose in Beverages." [Online]. Available: https://pineresearch.com/shop/kb/applications/laboratory-exercises/electrochemical-enzymatic-determination/. [Accessed: March 2016].

[18] T. Park, J. Choo, M. Lee, Y. S. Kim, E. K. Lee, H. S. Lee, "Enhancement of The Protein Loading Density by a Pre-Cleaning Process of a Gold Substrate: Confocal Laser Scanning Microscopic Study." *Anal Sci*., vol. 20, pp. 1255–1258, 2004.

[19] P. Rodríguez-Franco, Ll. Abad, F.X. Mu ˜noz-Pascual, M. Moreno, and E. Baldrich. "Effect of The Transducer's Surface Pre-Treatment on SPR Aptasensor Development." *Sensors and Actuators B: Chemical*, vol. 191, pp. 634-642, 2014.

[20] K. Niegelhell, S. Leimgruber, T. Grießer, C. Brand, B. Chernev, R. Schennach, G. Trimmel, and S. Spirk. "Adsorption Studies of Organophosphonic Acids on Differently Activated Gold Surfaces." *Langmuir*, vol. 32, no. 6, pp. 1550-1559, 2016.

[21] NanoSPR: Devices and accessories for Surface Plasmon Resonance, "Surface Plasmon Resonance Slide with Evaporated Au Film with Refractive Index 1.61." [Online]. Available: https://nanospr.com/surface-plasmon-resonance-slide-with-au-film/. [Accessed: 2025]

[22] V. Yesudasu, H. S. Pradhan, R. J. Pandya. "Recent Progress in Surface Plasmon Resonance Based Sensors: A Comprehensive Review." *Heliyon*, vol. 7, p. e06321, 2021.

[23] P. A. Van der Merwe, "Surface Plasmon Resonance." 2003.

[24] P. Steglich, G. Lecci, and A. Mai. "Surface Plasmon Resonance (SPR) Spectroscopy and Photonic Integrated Circuit (PIC) Biosensors: A Comparative Review." *Sensors (Basel)*, vol. 22, no. 8, p. 2901, 2022.

[25] J. A. Jones, L. A. Qin, H. Meyerson, II K. Kwon, T. Matsuda, and J. M. Anderson. "Instability of Self-Assembled Monolayers (SAM) as a Model Material System for Macrophage/FBGC Cellular Behavior." *J Biomed Mater Res A*, vol. 86, no. 1, pp. 261–268, 2008.

[26] X. Shi, L. Kuai, D. Xu, Y. Qiao, Y. Chen, B. Di, and P. Xu. "Surface Plasmon Resonance (SPR) for the Binding Kinetics Analysis of Synthetic Cannabinoids: Advancing CB1 Receptor Interaction Studies." *Int. J. Mol. Sci.*, vol. 26, no. 8, p. 3692, 2025.

[27] D. Capelli, V. Scognamiglio, and R. Montanari, "Surface Plasmon Resonance Technology: Recent Advances, Applications and Experimental Cases." *Trends in Analytical Chemistry,* vol. 163, p. 117079, 2023.

[28] A.K. Assaifan. "Thiol-SAM Concentration Effect on the Performance of Interdigitated Electrode-Based Redox-Free Biosensors." *Micromachines*, vol. 15, no. 10, p. 1254, 2024.

[29] Q.Q. Meng, X. Zhao, S.J. Chen, C.Y. Lin, Y.C. Ding, and Z.Y. Chen. "Performance Analysis of Surface Plasmon Resonance Sensor with High-Order Absentee Layer." *Chinese Phys. B,* vol. 26, p. 124213, 2017.

[30] G. Gauglitz. "Analytical Evaluation of Sensor Measurements." *Anal Bioanal Chem,* vol. 410, pp. 5–13, 2018.

[31] J. Homola. “Surface Plasmon Resonance Sensors for Detection of Chemical and Biological Species.”*Chem. Rev.* 108, 462−493, 2008

[32] M. Bakhshpour-Yücel, M. Küçük, E. T. Ozer, and B. Osman. “Nano-MIP Based SPR Sensor for Tetracycline Analysis in Milk Sample.” *Talanta Open,* vol. 11, p. 100417, 2025.

[33] N. Jendrike, A. Baumstark, U. Kamecke, C. Haug, and G. Freckmann. “ISO 15197: 2013 Evaluation of a Blood Glucose Monitoring System’s Measurement Accuracy.” *J. Diabetes Sci. Technol.,* vol. 11, no. 6, pp. 1275–1276, 2017.